ACS Macro Letters

Letter

pubs.acs.org/macroletters

Polymer-Grafted Nanoparticles with Precisely Controlled Structures

Yingbo Ruan,[†] Lei Gao,[‡] Dongdong Yao,[‡] Ke Zhang,[‡] Baoqing Zhang,[†] Yongming Chen,*[,§] and Chen-Yang Liu*[,†]

[†]Beijing National Laboratory for Molecular Sciences, CAS Key Laboratory of Engineering Plastics, Institute of Chemistry, the Chinese Academy of Sciences, Beijing 100190, China

[‡]Beijing National Laboratory for Molecular Sciences, State Key Laboratory of Polymer Physics and Chemistry, Institute of Chemistry, the Chinese Academy of Sciences, Beijing 100190, China

[§]Key Laboratory for Polymeric Composite and Functional Materials of Ministry of Education, Department of Polymer and Materials Sciences, School of Chemistry and Chemical Engineering, Sun Yat-Sen University, NO. 135, Xingang Xi Road, Guangzhou 510275, China

Supporting Information

ABSTRACT: Polymer-tethered nanoparticles with different geometric shapes are very useful fillers of polymer nanocomposites. Herein, a universal approach for the fabrication of such nanoparticles with precisely controlled shape and composition is reported. By microphase separation of poly(3-(triethoxysilyl)propyl methacrylate)-*block*-polystyrene (PTEPM-*b*-PS) in the presence of oligomers, o-TEPM (oT) and/or o-S (oS), followed by cross-linking and dispersion in PS solvent, precisely tailored PS-grafted nanoparticles were prepared. These particles include those with varied shapes but identical PS shells, particles with varied core sizes but the same PS shell, and particles with fixed shapes but varied PS shells. These particles are ideal model nanofillers to study the dynamics and reinforced mechanism of polymer nanocomposites.

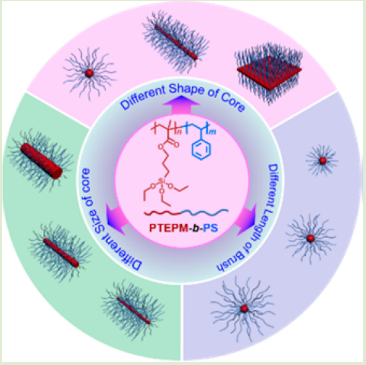

The dispersion of nanoparticles (NPs) in a polymer matrix, generating polymer nanocomposites, is a powerful method to improve the properties of polymer materials, such as electrical conductivity and mechanical and thermal properties.[1,2] The polymer−particle interactions and the spatial dispersion of nanoparticles have a significant impact on the properties of nanocomposites.[3] Surface chemical modification of nanoparticles, especially for grafting polymer chains on the surface of NPs, is the most important strategy to control NP dispersion in the polymer matrix.[4] Kumar and co-workers[5−7] studied the influence of structures of polymer-grafted nanoparticles (PGNPs) on their spatial distribution and how it affected their properties. Parameters such as grafting density, grafted chain length, matrix chain length, and loading volume, which affect NP dispersion, have been illustrated. Furthermore, solvent-free nanoparticle[8] and star polymers with many arms[9,10] have also been studied. However, most of the work in this area has focused on spherical PGNPs. Highly anisotropic NPs, such as carbon nanotubes, graphene, and clay, can achieve mechanical and electrical percolations at much lower loadings than spherical NPs.[11−13] No clear understanding of the effects of their surface-grafting factor on their properties has been reported. Moreover, the filled NPs in the literature include various materials, but they are not comparable because of the different chemical structures and size scales. Thus, the roles played by *NP shape and size* have not been fully realized. The problem is that there is no universal approach to prepare PGNPs with precisely defined shapes, cores, and shell sizes for use as model fillers for research. Thus, how to fabricate PGNPs with various cores and polymer chains that can be independently controlled is the basis of further work. In this study, a facile method of microphase separation of block copolymers (BCPs) in the presence of low molecular weight (MW) polymers was introduced to prepare PGNPs with precisely controlled structural parameters, including shape of the core, size of the core, and length of the grafted polymer.

Copolymers comprising two chemically immiscible blocks can self-assemble into various ordered nanoscale structures, such as spheres (S), cylinders (C), double gyroids (G), and lamellae (L),[14] which have been used to fabricate a variety of polymer nanomaterials.[15−17] Cross-linking the discontinuous domains, followed by dispersing in a good solvent of the non-cross-linked blocks, has become a new method (Assembly-Cross-link-Dispersion, ACD) to fabricate grafted core/shell nanoparticles.[18−20] Because microphase-separated structures of AB diblock copolymers are controlled by volume fractions, PGNPs with different core shapes (e.g., sphere, cylinder, and lamella) fabricated by the ACD method have different mass ratios of core to shell, indicating that the structural parameters of PGNPs cannot be independently controlled by the original

Received: June 19, 2015
Accepted: September 2, 2015
Published: September 9, 2015

DOI: 10.1021/acsmacrolett.5b00408
ACS Macro Lett. 2015, 4, 1067−1071

ACD method. Moreover, a series of block copolymers with different compositions have to be synthesized to prepare PGNPs with different structures. The microphase-separated morphology of block copolymers can also be controlled and changed by adding homopolymers, i.e., coassembly of copolymers with homopolymers.[21−23] Herein, a modified ACD method combining the original ACD method and the coassembly of AB diblock copolymers with oligomer A or B was developed to fabricate precisely defined PGNPs with not only fixed shapes but also parameters of core and shell size.

The modified ACD method for controlling the structural parameters is illustrated in Figure 1. The diblock copolymer is PTEPM-*b*-PS, and the corresponding oligomers are oT and oS. TEPM units containing trialkoxysilane groups may form cross-linked polysilsesquioxane networks under acidic or basic conditions. By adding either oT or oS to PTEPM-*b*-PS, the volume fractions of PTEPM and PS are tuned; therefore, the ordered microphase-separated structures are changed from one to the other. For example, as shown in Figure 1a, when oS is added to PTEPM-*b*-PS, the original morphology may change from L to C and finally to S. The oS may be removed easily in a near-theta solvent of PS after cross-linking the PTEPM domains. By this method, the core shape is tuned from one BCP precursor, while the content and length of the PS shell remain unchanged. When the BCP is blended with a certain amount of oT and oS mixture, whose ratio is the same as that of the two components of the BCP, two oligomers enter into the corresponding domains and increase their thickness, as shown in Figures 1c and 1d. Because of the blending with a constant TEPM/S ratio, the microphase morphology remains unchanged. After cross-linking, the oT merges into the core to increase the core thickness, whereas the PS remains after removal of the oS. By this method, PGNPs with fixed PS lengths but controlled core sizes are obtained. Furthermore, the PGNPs with the same core size but different PS lengths may be prepared, as shown in Figures 1e and 1f.

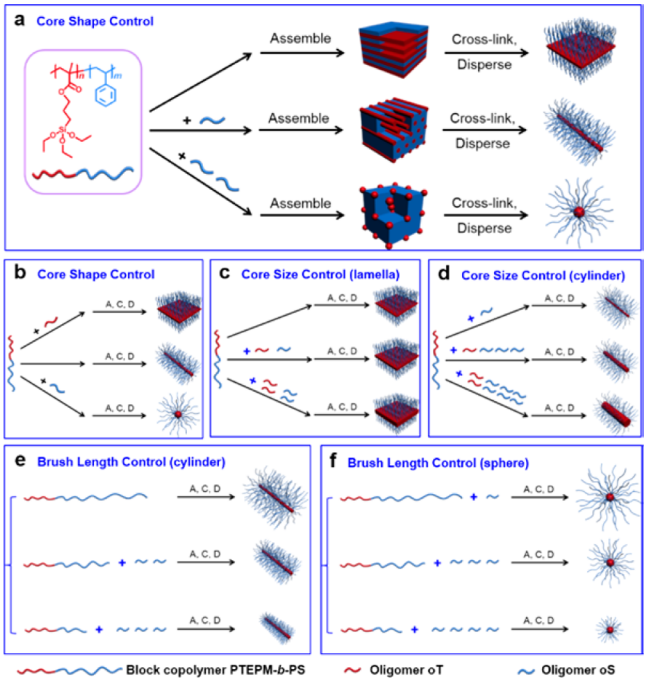

Figure 1. Schematic illustrations of fabrication of PGNPs with different structures by the Assembly-Cross-link-Dispersion (ACD method) of PTEPM-*b*-PS block copolymer and the corresponding oligomers, oT and/or oS, as discussed in the text. (a), (b) PGNPs with different core shapes; (c) lamellar PGNPs with different core thicknesses; (d) cylindrical PGNPs with different core diameters; (e) cylindrical PGNPs with different polymer brush lengths; (f) spherical PGNPs with different polymer brush lengths. A: Assembly of block copolymer and oligomers. C: Cross-linking of PTEPM domains. D: Dispersion of bulk materials.

A series of PTEPM-*b*-PS diblock copolymers with different compositions and narrow MW distributions (polydispersity index, PDI < 1.2) were synthesized by reversible addition−fragmentation chain-transfer (RAFT)-mediated radical polymerization. Oligomers oT and oS were also synthesized by RAFT polymerization. Experimental details are summarized in the Supporting Information (SI). The characteristics of the diblock copolymers and oligomers are collected in Table 1. Oligomers with lower MW, which have a higher diffusion coefficient, may improve the miscibility with the corresponding block in the copolymers.[21,24] Then the preparation of three sort of PGNPs was illustrated as follow: core shape control with the same shell, core size control with the same shape and shell, brush length control with the same core diameter.

$PTEPM_{38k}$-*b*-PS_{65k} self-assembled into a lamellar morphology as confirmed by the small-angle X-ray scattering (SAXS) curve and transmission electron microscopy (TEM) image (Figures S1a,d, respectively). When 50 or 150 wt % of oS (to the weight of copolymer) was blended with $PTEPM_{38k}$-*b*-PS_{65k}, cylindrical or spherical structures were obtained, respectively. In Figure S1, both the SAXS patterns of the films and the TEM images of the microtomed slices suggest the expected structures. The films with desired morphology were exposed to an atmosphere of hydrochloric acid for 12 h to induce the cross-linking reaction

Table 1. Characteristics of Block Copolymers and Oligomers Used in This Study

sample code[a]	block copolymers	M_n[b] (kg/mol)	copolymer PDI[c]	PS mass fraction (%)	morphology[d]
S47	$PTEPM_{48k}$-*b*-PS_{42k}	48-*b*-42	1.14	46.5	L
S70	$PTEPM_{48k}$-*b*-PS_{111k}	48-*b*-111	1.17	69.8	L
S63	$PTEPM_{38k}$-*b*-PS_{65k}	38-*b*-65	1.20	63.0	L
S71	$PTEPM_{38k}$-*b*-PS_{93k}	38-*b*-93	1.19	71.0	L
S80	$PTEPM_{38k}$-*b*-PS_{152k}	38-*b*-152	1.20	80.0	C
oT	o-$TEPM_{6k}$	6	1.10	0	--
oS	o-S_{6k}	6	1.06	100	--

[a]The number denotes the mass fraction of the PS block in the copolymer. [b]Calculated from the monomer conversion and the ratio of the two blocks from ^{1}H NMR spectra. [c]Polydispersity index, PDI = M_w/M_n, as obtained from size exclusion chromatography. [d]Microphase separation morphologies of block copolymer, L = alternating lamellae, C = hexagonal cylinders.

DOI: 10.1021/acsmacrolett.5b00408
ACS Macro Lett. 2015, 4, 1067−1071

of the PTEPM domains (Scheme S1). Then, the PGNPs and oS were dispersed in tetrahydrofuran (THF), a PS solvent. oS must be removed because it is not compatible with the matrix material (e.g., high molecular weight PS) used in the nanocomposites. The mixture of PGNPs and oS was refluxed in cyclohexane and then cooled to ambient temperature. PGNPs were separated from solution because of their poor solubility at ambient temperature, whereas oS remained dissolved in the solvent (see details in SI). Both TEM images (Figures 2a–c) and atomic force microscopy (AFM) height images (Figures S1g–l) show that PGNPs with different shapes were obtained. These PGNPs from PTEPM$_{38k}$-*b*-PS$_{65k}$ have the same PS shell length and content. Thus, three different shaped particles were obtained and characterized by thermogravimetric analysis (TGA) (Figure S2), which demonstrated identical degradation behaviors, implying that the shaped PGNPs have the same core and shell composition. The characteristics of the particles, including core size and mass fraction, PS shell molar mass, and graft density, are collected in Table 2 (Series 1). Thus, the PGNPs with identical compositions but different shapes can be prepared by the procedure shown in Figure 1a.

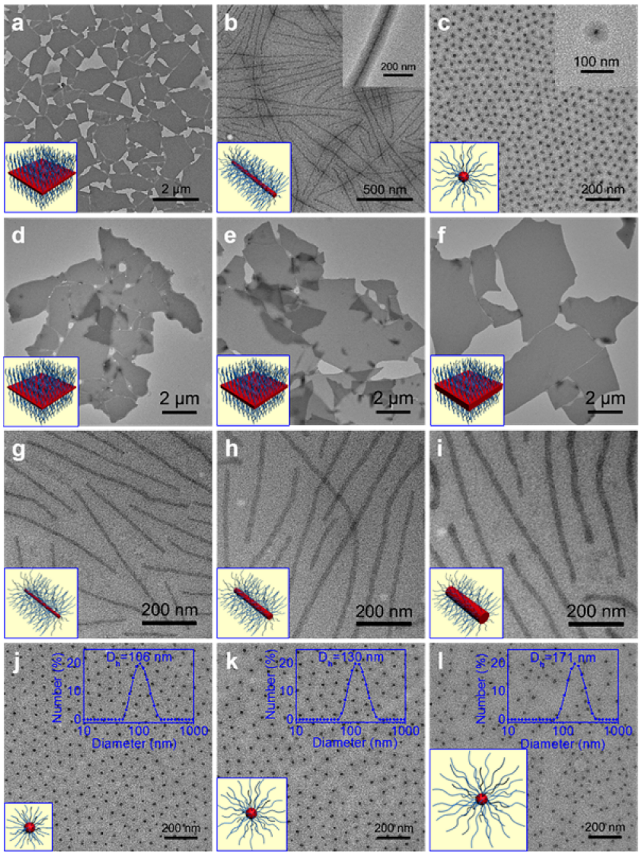

Figure 2. TEM images of isolated PGNPs with different structures. (a) lam-65k, (b) cyl-65k, and (c) sph-65k are PGNPs with different shapes but the same brush length. (d) lam-18 nm-42k, (e) lam-21 nm-42k, and (f) lam-27 nm-42k are lamellar PGNPs with different core thicknesses but the same brush length. (g) cyl-26 nm-111k, (h) cyl-32 nm-111k, and (i) cyl-40 nm-111k are cylindrical PGNPs with different core diameters but the same brush length. (j) sph-25 nm-65k, (k) sph-25 nm-93k, and (l) sph-25 nm-152k are spherical PGNPs with different brush lengths but the same core size (inset shows the size distribution of PGNPs in solvent measured by DLS).

Another series of PGNPs with the same PS shells but different shapes were obtained from PTEPM$_{38k}$-*b*-PS$_{152k}$, which has a C phase. By adding an optimized amount of oT (23 wt %) or oS (100 wt %), the ACD method resulted in lamellar or spherical phases (Figure S3) as expected (Figure 1b). Thereafter, different shaped PGNPs with PS$_{152k}$ shells were prepared, and their characteristics are collected in Table 2 (Series 2). Note that the content of the lamellar core was different by this method because the blended oT was merged into the cores.

The PTEPM$_{48k}$-*b*-PS$_{42k}$ copolymer is used as the starting material, which forms the lamellar morphology in bulk (Figure S4). When the copolymer was blended with a mixture of oT (35 wt %) and oS (31 wt %), whose ratio is the same as that of the block copolymer, the microphase-separated structures remain, but the blended oligomers increase their periodic length. After cross-linking, the oT merged into the cores, whereas oS was removed. As a result, the blended oT gave an increase of core thickness from 18 to 21 nm as given by the SAXS data (Figure S4). Further blending with more oT (83 wt %) and oS (74 wt %) resulted in the structure with a core thickness of 27 nm. Thereafter, the obtained lamellar PGNPs showed well-defined thicknesses as shown by the TEM (Figures 2d–f) and AFM (Figures S4g–i) images. These platelets have identical PS shells but varied core thicknesses. Controlling the core diameter of cylindrical PGNPs is similarly conducted with PTEPM$_{48k}$-*b*-PS$_{111k}$. The data in Figure S5 show an increase in the periodic length upon blending both oT and oS. The dispersed cylinders show an obvious increase in the core diameter from 26 to 40 nm (Figures 2g–i). However, all of the particles have the same PS length, PS$_{111k}$. The characteristics of both the lamellar and cylindrical PGNPs are summarized in Table 2 (Series 3 and 4).

Three PTEPM-*b*-PS copolymers, PTEPM$_{38k}$-*b*-PS$_x$ (x = 65k, 93k, 152k), were applied. PTEPM$_{38k}$-*b*-PS$_{152k}$ with the longest PS block forms a cylindrical phase (Figure S6). It was observed that blending PTEPM$_{38k}$-*b*-PS$_{65k}$ and PTEPM$_{38k}$-*b*-PS$_{93k}$ with 50 and 25 wt % oS, respectively, to ensure the TEPM/S ratio is the same as the PTEPM$_{38k}$-*b*-PS$_{152k}$, may form the C phase (Figure S6). Therefore, three final cylinders with the same diameters with different PS lengths ranging from 65k to 93k to 152k were obtained. A similar adjustment was also applied to spheres. The same BCPs were applied and mixed with different amounts of oS, i.e., PTEPM$_{38k}$-*b*-PS$_{65k}$ + 280 wt % oS, PTEPM$_{38k}$-*b*-PS$_{93k}$ + 200 wt % oS, and PTEPM$_{38k}$-*b*-PS$_{152k}$ + 100 wt % oS, to maintain the total TEPM/S ratio as a constant. Because of the greatly increased volume ratio of the PS phase, three blended samples formed the S phase as shown in Figure S7. After cross-linking the core and removing oS, monodispersed spheres with the same diameters but different PS lengths were obtained (Figures 2j–l). The diameters of the spherical PGNPs in THF, monitored by dynamic light scattering (Figures 2j–l, insets), increased with increasing PS block length. The characteristics of the cylindrical and spherical PGNPs are collected in Table 2 (Series 5 and 6). Six PGNPs of these two series were prepared from the same group of BCPs with the aid of oS. Each series had the same shape but varied in PS length.

The structural parameters of the six series of PGNPs prepared in this paper are listed in Table 2. The above results demonstrate that core/shell PGNPs may be tailored with the aid of oT and/or oS. Advantages of the modified ACD method to create grafted nanoparticles are obvious. In the previous BCP

DOI: 10.1021/acsmacrolett.5b00408
ACS Macro Lett. 2015, 4, 1067–1071

Table 2. Composition of Assembly Films and the Structural Parameters of Six Series of PGNPs

series (parameters adjusted)	composition of assembly films[a]	PGNPs[b] (core−brush MW)	core size D^c (nm)		mass fraction of core (%)	graft density (chains/nm^2)
			D_{SAXS}[d]	D_{TEM}[e]		
series 1 (shape)	neat S63	lam-65k	14	--	27.0	0.134
	S63 + 50% oS	cyl-65k	23	22	27.0	0.109
	S63 + 150% oS	sph-65k	28	26	27.0	0.090
series 2 (shape)	S80 + 23% oT	lam-152k	22	--	25.0	0.096
	neat S80	cyl-152k	25	24	13.4	0.118
	S80 + 100% oS	sph-152k	25	24	13.4	0.081
series 3 (lamellae thickness)	neat S47	lam-18 nm-42k	18	--	41.5	0.138
	S47 + 35% oT + 31% oS	lam-21 nm-42k	21	--	54.0	0.095
	S47 + 83% oT + 74% oS	lam-27 nm-42k	27	--	64.4	0.078
series 4 (cylinder diameter)	S70 + 50% oS	cyl-26 nm-111k	26	24	21.1	0.098
	S70 + 15% oT + 110% oS	cyl-32 nm-111k	32	30	28.6	0.080
	S70 + 31% oT + 175% oS	cyl-40 nm-111k	40	37	35.1	0.073
series 5 (brush length for cylinders)	neat S80	cyl-25 nm-152k	25	24	13.4	0.118
	S71 + 25% oS	cyl-24 nm-93k	24	23	20.1	0.112
	S63 + 50% oS	cyl-23 nm-65k	23	22	27.0	0.109
series 6 (brush length for spheres)	S80 + 100% oS	sph-25 nm-152k	25	24	13.4	0.081
	S71 + 200% oS	sph-25 nm-93k	25	25	20.1	0.081
	S63 + 280% oS	sph-25 nm-65k	25	24	27.0	0.080

[a]Oligomer content expressed as a weight percentage of the copolymer. [b]lam: lamella; cyl: cylinder; sph: sphere. [c]Thickness of the lamellae, diameter of the cylinders and spheres. [d]Calculated from the SAXS spectrum. [e]Determined from the TEM images of the isolated spherical or cylindrical PGNPs. For each sample, more than 100 particles were measured to obtain the average size. The calculation method of structural parameters can be found in the SI.

approach without oligomers, factors such as shape, core, and shell size were changed simultaneously because of the nature of block copolymer microphase separation. Now, these factors may be independently tuned in the presence of oT and/or oS (Table 2). Compared to grafting polymerization from nanoparticles with prefixed shapes,[25,26] which typically involves a reaction on the solid surface, the cores are formed in situ from one segment of BCPs, and the shell polymers are inherited from another segment. The distribution of the number of chains per particle (for spherical PGNPs) and the spatial distribution of the graft points on the particle are very uniform because the assembly is in a thermodynamic equilibrium state. The final shape of the PGNPs is governed by the volume ratio of the two polymers, which are contributed by either the composition of the BCPs or the blended oligomers. Furthermore, PGNPs with bimodal brushes (of two different lengths) or mixed brushes (of two different polymers) can be easily achieved by using a mixture of two precursor copolymers.

In summary, a facile and versatile method to prepare PGNPs with precisely controlled structural factors is presented. The ACD method has extended the structural parameter space of PGNPs in terms of nanoparticle shape and size, grafting density, and brush length and composition. Further possibilities can be explored by changing the structure of the diblock copolymers and the additive amounts of oligomers. Furthermore, the strategies used herein can be easily applied to other copolymer systems once they contain a component on which cross-linking reactions can occur. In terms of application, these precisely tailored PGNPs are ideal model fillers for polymer nanocomposites, which are likely to provide a full understanding of the structure−property relationship of nanocomposites. For example, how the packing, orientation and percolation of nonspherical PGNPs contribute to the reinforcement of PGNPs under melt and solid states of the polymeric materials will be elucidated. Additionally, by eliminating chemical and physical differences, the effect of the shape of fillers on the dynamics (e.g., diffusion, viscoelasticity) of polymer composites can be investigated.

■ ASSOCIATED CONTENT

Supporting Information

The Supporting Information is available free of charge on the ACS Publications website at DOI: 10.1021/acsmacrolett.5b00408.

Experimental details; characteristics of block copolymers; additional TEM images and SAXS data of bulk materials and TEM and AFM images of the isolated PGNPs with different structures; calculation method of structural parameters (PDF)

■ AUTHOR INFORMATION

Corresponding Authors

*E-mail: chenym35@mail.sysu.edu.cn.

*E-mail: liucy@iccas.ac.cn.

Notes

The authors declare no competing financial interest.

■ ACKNOWLEDGMENTS

This work is supported by the NSFC (No. 21174153), National Basic Research Program of China (973 Program, No. 2014CB643601), and the Guangdong Natural Science Foundation (No. 2014A030312018).

■ REFERENCES

(1) Paul, D. R.; Robeson, L. M. *Polymer* **2008**, *49*, 3187.

(2) Jancar, J.; Douglas, J. F.; Starr, F. W.; Kumar, S. K.; Cassagnau, P.; Lesser, A. J.; Sternstein, S. S.; Buehler, M. J. *Polymer* **2010**, *51*, 3321.

(3) Pandey, Y. N.; Papakonstantopoulos, G. J.; Doxastakis, M. *Macromolecules* **2013**, *46*, 5097.

DOI: 10.1021/acsmacrolett.5b00408
ACS Macro Lett. 2015, 4, 1067−1071

(4) Krishnamoorti, R. *MRS Bull.* **2007**, *32*, 341.
(5) Akcora, P.; Liu, H.; Kumar, S. K.; Moll, J.; Li, Y.; Benicewicz, B. C.; Schadler, L. S.; Acehan, D.; Panagiotopoulos, A. Z.; Pryamitsyn, V.; Ganesan, V.; Ilavsky, J.; Thiyagarajan, P.; Colby, R. H.; Douglas, J. F. *Nat. Mater.* **2009**, *8*, 354.
(6) Moll, J. F.; Akcora, P.; Rungta, A.; Gong, S.; Colby, R. H.; Benicewicz, B. C.; Kumar, S. K. *Macromolecules* **2011**, *44*, 7473.
(7) Maillard, D.; Kumar, S. K.; Fragneaud, B.; Kysar, J. W.; Rungta, A.; Benicewicz, B. C.; Deng, H.; Brinson, L. C.; Douglas, J. F. *Nano Lett.* **2012**, *12*, 3909.
(8) Yu, H. Y.; Koch, D. L. *J. Rheol.* **2014**, *58*, 369.
(9) Vlassopoulos, D.; Fytas, G.; Pakula, T.; Roovers, J. *J. Phys.: Condens. Matter* **2001**, *13*, R855.
(10) Vlassopoulos, D. *J. Polym. Sci., Part B: Polym. Phys.* **2004**, *42*, 2931.
(11) Bauhofer, W.; Kovacs, J. Z. *Compos. Sci. Technol.* **2009**, *69*, 1486.
(12) Kuilla, T.; Bhadra, S.; Yao, D.; Kim, N. H.; Bose, S.; Lee, J. H. *Prog. Polym. Sci.* **2010**, *35*, 1350.
(13) Okada, A.; Usuki, A. *Macromol. Mater. Eng.* **2006**, *291*, 1449.
(14) Bates, F. S.; Fredrickson, G. H. *Annu. Rev. Phys. Chem.* **1990**, *41*, 525.
(15) Rodriguezhernandez, J.; Checot, F.; Gnanou, Y.; Lecommandoux, S. *Prog. Polym. Sci.* **2005**, *30*, 691.
(16) Yuan, J.; Xu, Y.; Muller, A. H. *Chem. Soc. Rev.* **2011**, *40*, 640.
(17) Walther, A.; Muller, A. H. *Chem. Rev.* **2013**, *113*, 5194.
(18) Liu, G. J.; Qiao, L. J.; Guo, A. *Macromolecules* **1996**, *29*, 5508.
(19) Zhang, K.; Gao, L.; Chen, Y. M. *Macromolecules* **2007**, *40*, 5916.
(20) Nandan, B.; Horechyy, A. *ACS Appl. Mater. Interfaces* **2015**, *7*, 12539.
(21) Tanaka, H.; Hasegawa, H.; Hashimoto, T. *Macromolecules* **1991**, *24*, 240.
(22) Winey, K. I.; Thomas, E. L.; Fetters, L. J. *J. Chem. Phys.* **1991**, *95*, 9367.
(23) Gao, L.; Zhang, K.; Chen, Y. M. *Polymer* **2011**, *52*, 3681.
(24) Hashimoto, T.; Tanaka, H.; Hasegawa, H. *Macromolecules* **1990**, *23*, 4378.
(25) Tao, P.; Li, Y.; Rungta, A.; Viswanath, A.; Gao, J.; Benicewicz, B. C.; Siegel, R. W.; Schadler, L. S. *J. Mater. Chem.* **2011**, *21*, 18623.
(26) Rungta, A.; Natarajan, B.; Neely, T.; Dukes, D.; Schadler, L. S.; Benicewicz, B. C. *Macromolecules* **2012**, *45*, 9303.

DOI: 10.1021/acsmacrolett.5b00408
ACS Macro Lett. 2015, 4, 1067−1071